NUMERICAL SIMULATION OF 3D TRANSONIC FLOW IN A COMPRESSOR ROTOR

K.C. Ng,* M.Z. Yusoff,** and T.F. Yusaf***

Abstract

This paper presents a new computational fluid dynamics (CFD) code developed at Universiti Tenaga Nasional for the numerical computation of transonic laminar flow in a compressor rotor. The 3D computational code solves the unsteady Navier-Stokes equations (NSE) on unstructured hexahedral mesh by using second-order accurate central differencing scheme on both convective and diffusive terms. Artificial damping terms are added to control the stability of the numerical scheme, and the explicit multistage Runge-Kutta time-integration technique is performed to solve the unsteady NSE. This paper discusses the simulation of compressible flow field in an axial-flow compressor rotor using the newly developed CFD code. The predicted flow is then compared with the results obtained from the commercial code, *CFX-5*, as well as experimental data; good agreement is found.

Key Words

CFD, Navier-Stokes equations, CFX, DFVLR compressor rotor

1. Introduction

The system of Navier-Stokes equations (NSE) is the most common mathematical model used to predict the flow physics in general domain. However, except for very few special cases, there is no analytical solution available for this mathematical model, and one has to resort to numerical approach. The art of solving these nonlinear partial differential equations is known as computational fluid dynamics (CFD), which has been an active area of research for the past few decades.

The numerical computation of fluid flow in turbomachines has attracted considerable attention from design engineers in the area of turbomachinery. In many practical flow problems in turbomachines, the detailed flow field information can only be retrieved by using CFD, because detailed measurement in rotating passage of turbomachinery components is cumbersome, and in many instances impossible. Transonic flow through the compressor rotor is probably one of the most difficult problems in CFD, and hence it represents a considerable challenge for the development of numerical schemes. The relative flow may become supersonic near the throat region, and it represents the formation of shock waves, which could be extending from mid-span of the rotating blade towards the tip, and interact with blade surface boundary layers and lead to flow separation. For engineering applications, it is an optimal choice to solve the Navier-Stokes equations for simulation of flow through complex domain with effective convergence acceleration schemes. The multistage Runge-Kutta scheme developed by Jameson *et al.* [1], coupled with local time stepping and implicit residual averaging, has been considered an effective tool in CFD applications for solving turbomachinery flow problems [2, 3]. Structured mesh may be employed, provided the flow domain is not sophisticated that mapping of face elements is possible [2, 4, 5]. Notwithstanding this, by considering the incompetence of structured mesh in discretizing a truly complex flow domain, researchers have utilized unstructured grid in turbomachinery applications [3, 6].

This paper presents the development and validation of a new, unstructured hexahedral, 3D CFD solver, and applies it to the well-known DFVLR transonic rotor. In Section 2, the numerical background of the mathematical model will be briefly discussed. The new CFD solver will then be used to compute the complex flow field in a transonic axial compressor rotor, as presented in Section 3. The accuracy of the new solver will be validated against experimental data as well as predictions from the commercial code, *CFX-5*, which is prominent in the area of turbomachinery.

2. Numerical Methods

2.1 The Governing Equations

The three-dimensional continuity, x-, y- and z-momentum, and energy equations describing the flow of a compressible

* O.Y.L. R&D Center, Lot 4739, Jalan BRP 8/2, Taman Bukit Rahman Putra, 47000 Sungai Buloh, Selangor Darul Ehsan, Malaysia; e-mail: ngkhaiching2000@yahoo.com

** Universiti Tenaga Nasional, Km7, Jalan Kajang-Puchong, 43009 Kajang, Selangor, Malaysia; e-mail: zamri@uniten.edu.my

*** FOES, University of Southern Queensland, Toowoomba, 4350 QLD, Australia; e-mail: talal@uniten.edu.my

Recommended by Prof. Behrooz Fallahi
(paper no. 205-4495)

fluid expressed in strong conservation form in the x-, y-, z-Cartesian co-ordinate system may be written as:

$$\frac{\partial \underline{W}}{\partial t} + \frac{\partial \underline{F}}{\partial x} + \frac{\partial \underline{G}}{\partial y} + \frac{\partial \underline{H}}{\partial z} = \underline{J} \tag{1}$$

where:

$$\underline{W} = \begin{pmatrix} \rho \\ \rho u \\ \rho v \\ \rho w \\ \rho e_0 \end{pmatrix}; \quad \underline{F} = \begin{pmatrix} \rho u \\ \rho u^2 + P - \tau_{xx} \\ \rho uv - \tau_{xy} \\ \rho uw - \tau_{xz} \\ \rho u h_0 + Q_x - \Phi_1 \end{pmatrix}$$

$$\underline{G} = \begin{pmatrix} \rho v \\ \rho uv - \tau_{yx} \\ \rho v^2 + P - \tau_{yy} \\ \rho uw - \tau_{yz} \\ \rho v h_0 + Q_y - \Phi_2 \end{pmatrix}; \quad \underline{H} = \begin{pmatrix} \rho w \\ \rho uw - \tau_{zx} \\ \rho vw - \tau_{zy} \\ \rho w^2 + P - \tau_{zz} \\ \rho w h_0 + Q_z - \Phi_3 \end{pmatrix}$$

$$\underline{J} = \begin{pmatrix} 0 \\ 0 \\ \rho(2w\varpi_x + y\varpi_x^2) \\ \rho(-2v\varpi_x + z\varpi_x^2 \\ 0 \end{pmatrix}$$

$\underline{W}$ is known as the conserved variables; $\underline{F}$, $\underline{G}$, and $\underline{H}$ are the overall fluxes in x-, y-, z-directions respectively. $\underline{J}$ represents the source terms. Q_x, Q_y, and Q_z are heat transfer rates, and Φ_1, Φ_2, and Φ_3 are the viscous dissipation terms. ϖ_x is the angular speed about the x-axis (rad/s).

2.2 Spatial Discretization

The five equations of motion are discretized in finite volume form on each of the hexahedral cells with all the flow variables stored at the vertex. Fig. 1 illustrates the location of cell J, which is defined as any cells attached to node K. The flow variables are assumed to exhibit a piecewise linear variation over the cell faces (represented by superscript $\overline{\overline{\ }}$), and the convective flux sum of a given cell takes the following form:

$$flux_{cell\,J,convective} = \sum_{face=1}^{6} (\overline{\overline{F_C}} \cdot \underline{dA_x} + \overline{\overline{G_C}} \cdot \underline{dA_y} + \overline{\overline{H_C}} \cdot \underline{dA_z})\,|_{face} \tag{2}$$

The flux in cell J is then distributed to the surrounding nodes, denoted by $\underline{R}_{nodeK(convective)}$. For example:

$$\underline{R}_{nodeK(convective)} = \sum_{J=1}^{A} flux_{cell J,convective} \tag{3}$$

where A is defined as the total number of cells attached to node K. For example, by considering the arrangement of cells as illustrated in Fig. 1, $A = 8$ for each interior cell surrounding node K.

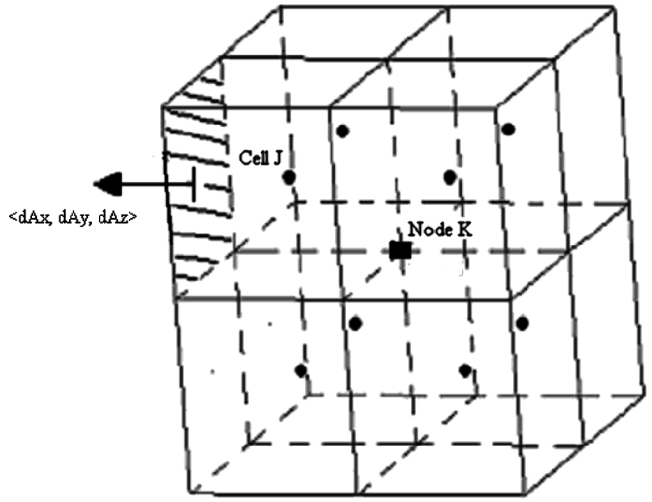

Figure 1. The compact stencil of hexahedral cells.

To evaluate the viscous flux, one must determine the derivative terms in each cell, as viscous terms are expressed in second-order form. Due to the fact that the variables are assumed to be piecewise linear, the derivative terms are piecewise constant over the cell, as denoted by:

$$\left(\frac{\partial \phi}{\partial x}\right)_{cell J} = \frac{1}{VOL_J} \sum_{face=1}^{6} \overline{\overline{\phi}}.dA_x\,|_{face} \tag{4}$$

Using this cell derivative, which is assumed to be constant throughout the cell, the second derivative at node K is evaluated by:

$$\frac{\partial}{\partial x}\left(\frac{\partial \phi}{\partial x}\right)_{nodeK} = \frac{1}{VOL_K} \sum_{J=1}^{A} \sum_{f=1}^{P} \left(\frac{\partial \phi}{\partial x}\right)_{cell_J} dA_{x,f} \tag{5}$$

in which P dictates the number of faces that are not attached to node K in a general hexahedral cell, VOL_J is the cell volume, and VOL_K is the total volume attached to node K. By adopting the same procedure in evaluating the viscous laminar fluxes, denoted by the subscript L, one should have:

$$\underline{R}_{nodeK(viscous,L)} = \sum_{J=1}^{A} \sum_{f=1}^{P} \overline{\overline{F_{L,cell J}}} \cdot \underline{dA_{x,f}} + \overline{\overline{G_{L,cell J}}} \cdot \underline{dA_{y,f}} + \overline{\overline{H_{L,cell J}}} \cdot \underline{dA_{z,f}} \tag{6}$$

Assembling all the fluxes, one should obtain:

$$\underline{R}_K = -\underline{R}_{nodeK(convective)} + \underline{R}_{nodeK(viscous,L)} + \underline{J}.VOL_K \tag{7}$$

2.3 Artificial Viscosity

In order to maintain the stability of the current time-marching algorithm, the fluxes computed using the central differencing scheme proposed in the previous section require the coupling of artificial viscosity, as suggested by Dawes [3]:

$$\underline{D}_K = \left[AV2 + AVA \times V_K^{\frac{2}{3}} \times \left| \frac{\nabla^2 P}{4P} \right| \right] a_0 \times \Delta L \times \nabla^2 \underline{W} \times V_K \tag{8}$$

where $\underline{W}$ represents the seven conserved variables, ΔL is the mean mesh spacing over the cell, a_0 is the velocity scale (stagnation speed of sound), and $VOL_K^{\frac{2}{3}} \times \left| \frac{\nabla^2 P}{4P} \right|$ is the pressure switch. The pressure switch uses a true Laplacian of static pressure, which has been assembled in three coordinate directions. In application, $AV2$ is set to 0.005 to 0.01 and AVA to 0.5. Equation (7), after the addition of artificial viscosity, is integrated with respect to time by means of a four-stage Runge-Kutta time stepping scheme, as proposed by Jameson *et al.* [1].

2.4 Boundary Conditions

At inlet boundary, absolute total pressure, absolute total temperature, and two flow angles are fixed, and the static pressure is extrapolated from the interior if the inflow is subsonic. Otherwise, all variables are specified. At exit, if the outflow is subsonic, only the static pressure is fixed, and other flow variables are extrapolated from the interior. Zeroth-order extrapolation technique is used. If the exit flow is supersonic, all the variables are extrapolated from the interior.

The periodicity condition on the bounding nodes is easily satisfied by treating the calculating nodes on each of the periodic surfaces as if they are interior ones, by assuming that all properties are equal for corresponding nodes on each of the periodic surfaces. Adiabatic and no-slip conditions are imposed at wall boundary to evaluate the velocity/temperature gradient near the wall to account for the effect on boundary layer. This appears as an additional source term added to nodes at/adjacent to the wall. Otherwise, the solver will assume inviscid simulation to be performed and the normal gradient of velocity component will be removed in evaluating the convective fluxes.

3. Application to DFVLR Transonic Compressor Rotor

The code is applied to the study of the three-dimensional flow-field in the axial flow single-stage transonic compressor rotor located at DFVLR. The objective here is to demonstrate the accuracy of the present solver as compared to the experimental data and results obtained from the commercial CFD code, *CFX-5*.

The compressor rotor has an inlet tip diameter of 0.4 m, 28 blades per row, a hub-tip ratio of 0.5, and tip solidity of 1.34. The design mass flow rate is 17.1 kg/s rotating at 20260 rpm about the x-axis in clockwise direction. The mesh employed is relatively coarse, consisting of 13294 cells and 15228 nodes per flow passage with crude refinement in zone near to the casing, hub, and blade. No attempt was performed to resolve the tip leakage flow. Similar mesh was used in both the present solver and *CFX-5*, as illustrated in Fig. 2 showing the surface mesh of the complete DFVLR compressor rotor.

The flow equations were solved in rotating frame of reference with appropriate Coriolis and centripetal force terms, and it was run until convergence with time factor, FT, of 0.5. The relative inflow Mach number varies from around 0.7 to about 1.4 towards the casing. Figs. 3–5 illustrates the predicted relative Mach number at the blade-to-blade plane of $z = 120$ mm, $z = 140$ mm, and $z = 150$ mm respectively. At $z = 120$ mm, the flow accelerates to just sonic near the leading edge and decelerates abruptly to Mach 0.5 across the shock wave represented by *CFX-5*, which is not quite well resolved using the current solver. At $z = 140$ mm and $z = 150$ mm, the relative inflow is supersonic and a well-resolved oblique shock forms at a region slightly downstream of the leading edge as predicted by the current solver. Furthermore, current prediction reveals that there is another shock wave originating from the leading edge that comes into interaction with the internal flow field. *CFX-5* tends to smear the leading-edge-shock, probably due to the excessive numerical diffusion inherited from the spatial differencing scheme. In general, by

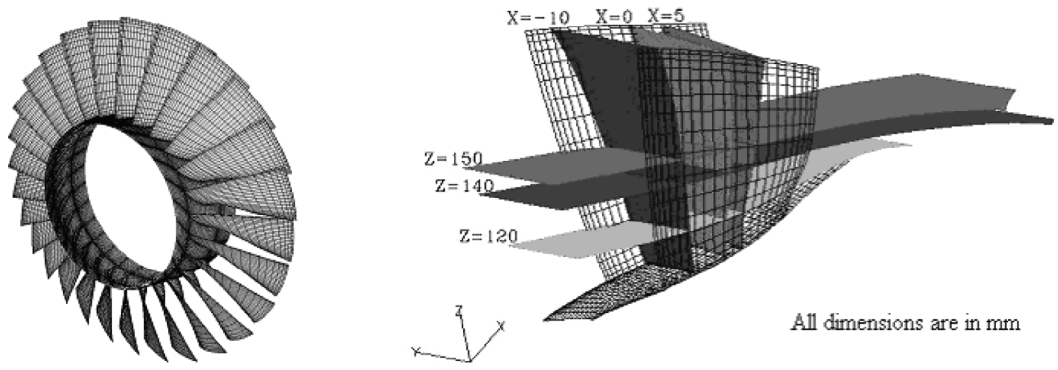

Figure 2. Surface mesh for the DFVLR compressor rotor with cutting planes established for presentation of results.

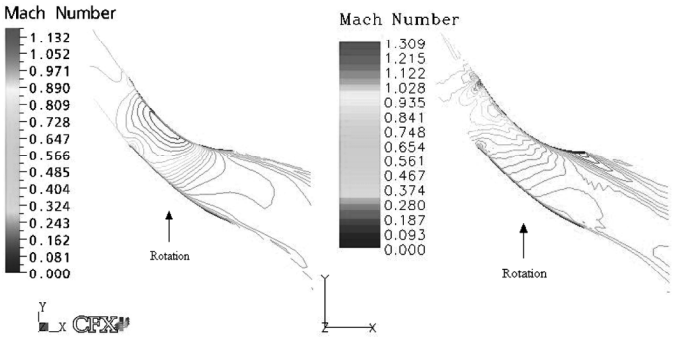

Figure 3. Comparisons of Mach contours at $z = 120\,\text{mm}$ using *CFX-5* (left) and the current solver (right).

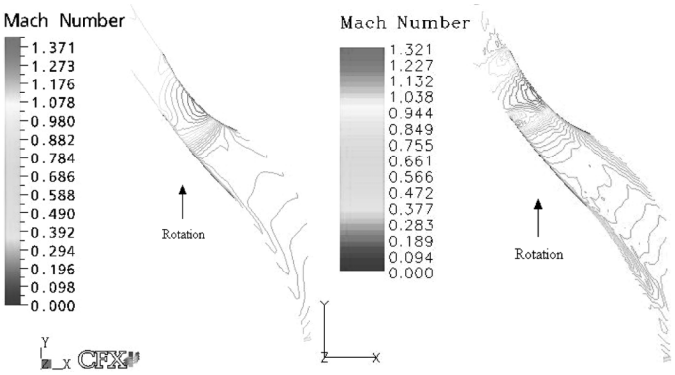

Figure 4. Comparisons of Mach contours at $z = 140\,\text{mm}$ using *CFX-5* (left) and the current solver (right).

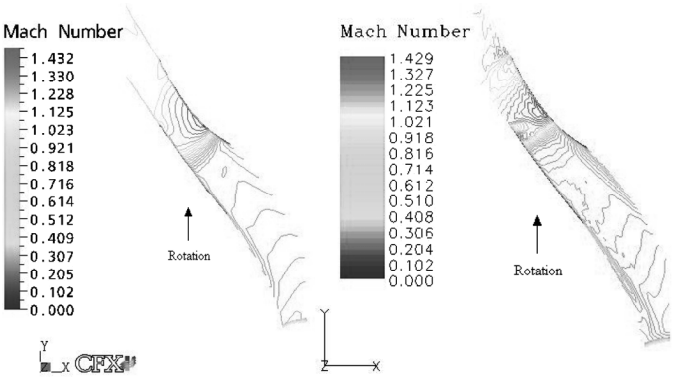

Figure 5. Comparisons of Mach contours at $z = 150\,\text{mm}$ using *CFX-5* (left) and the current solver (right).

considering the coarseness of the mesh, the resolution of the shock pattern is found to be satisfactory.

Figs. 6–8 present the pressure distribution at the cross-flow plane of $x = 0\,\text{mm}$, $x = -10\,\text{mm}$, and $x = 5\,\text{mm}$ respectively and illustrate clearly the shock patterns between the rotating blades. At $x = -10\,\text{mm}$, two shock surfaces were predicted from the current solver as well as *CFX-5*: the first shock surface extends from the hub-suction surface corner to the casing, which corresponds to the leading-edge-shock, and the second corresponds to the shock surface

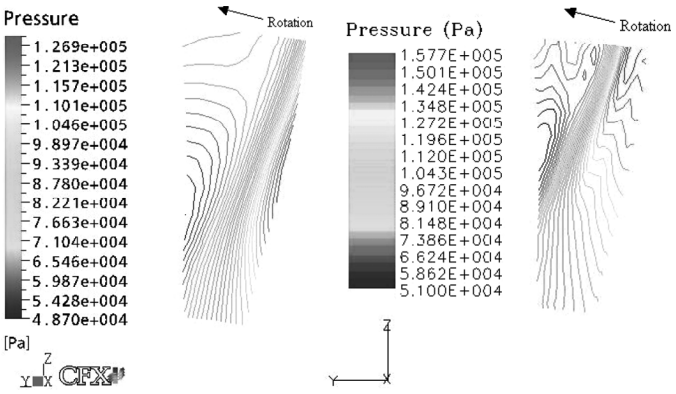

Figure 6. Comparisons of static pressure contours at $x = 0.0\,\text{mm}$ using *CFX-5* (left) and the current solver (right).

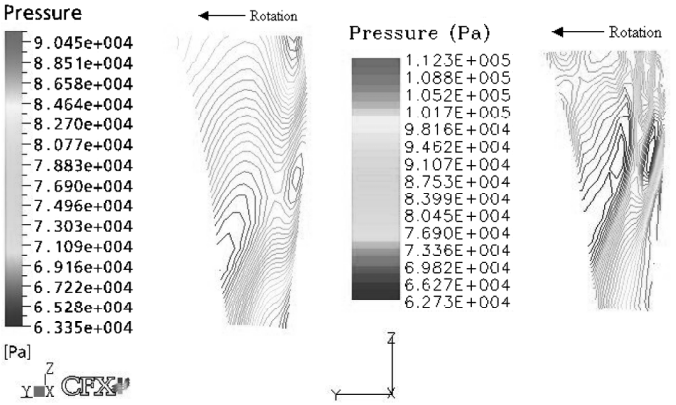

Figure 7. Comparisons of static pressure contours at $x = -10.0\,\text{mm}$ using *CFX-5* (left) and the current solver (right).

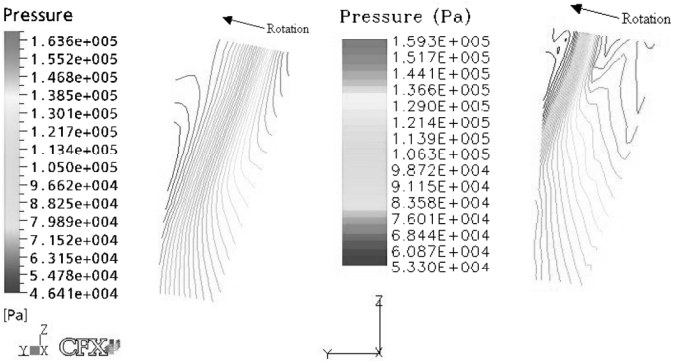

Figure 8. Comparisons of static pressure contours at $x = 5.0\,\text{mm}$ using *CFX-5* (left) and the current solver (right).

attached to the pressure side of the blade surface slightly downstream from the leading edge. At $x = 0\,\text{mm}$ and $x = 5\,\text{mm}$, the shock surface causes a significance pressure drop from the pressure to suction blade surface, impinging the suction blade surface and the casing as predicted by the

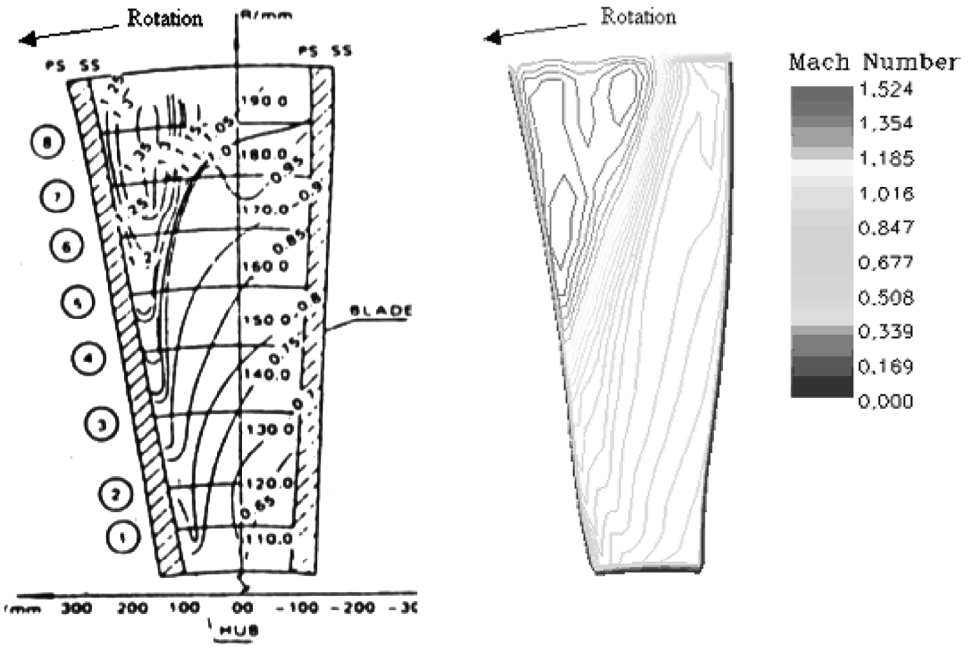

Figure 9. Comparisons of Mach contours at $x = 0.0$ mm predicted using the present solver (right) with experimental data (left) (experiment reproduced from Dawes [2]).

current solver. However, *CFX-5* predicted the shock to be formed slightly downstream, and it is relatively smeared as compared with the shock representation by the current solver. The predicted and measured contours of relative Mach number in the cross-flow plane of $x = 0$ mm are compared in Fig. 9. By comparing the location of the shock wave and spatial extent of the high Mach number region, we see that the agreement between the measurement and predictions is reasonably good.

4. Conclusion

In the present work, a three-dimensional unstructured hexahedral CFD solver was developed and the numerical methods used to solve the Navier-Stokes equations were described.

Transonic flow past through the DFVLR transonic compressor rotor was computed using the current solver. The results were compared with the commercial code, *CFX-5*, and reasonably good agreements have been found. The solution is susceptible to wiggles in certain flow region due to the embedded character of the current differencing scheme. However, it is believed that the solver will serve as a valuable simulation tool to investigate the compressible flow field in complex geometry.

Acknowledgement

The current work was performed while the first author was in residence at Universiti Tenaga Nasional, Malaysia. This project is funded by the Ministry of Science Technology and Innovation (MOSTI), Malaysia, under IRPA Grant no. 09-99-03-0013-EA001 and UNITEN Internal Research Grant no. J510010026.

References

[1] A. Jameson, W. Schmidt, & E. Turkel, Numerical solutions of the Euler equations by finite volume methods using Runge-Kutta time stepping schemes, AIAA Paper no. 81–1259, *14th Fluid and Plasma Dynamics Conf.*, Palo Alto, CA, June 23–25, 1981, 15.

[2] W.N. Dawes, A numerical analysis of the three-dimensional viscous flow in a transonic compressor rotor and comparison with experiment, *Journal of Turbomachinery*, *109*, 1987, 83–90.

[3] W.N. Dawes, The practical application of solution-adaption to the numerical simulation of complex turbomachinery problems, *Progress in Aerospace Science*, *29*, 1992, 221–269.

[4] M. Despotovic, M. Babic, D. Milovanovic, & V. Sustercic, Numerical simulation of complex 3D compressible viscous flows through rotating blade passages, *Theoretical and Applied Mechanics*, *30*(1), 2003, 55–82.

[5] J. Yao & X. Zhou, Computation of flow in a compressor blade row by a third order accurate high resolution scheme, *AIAA-1998-3561*, *34th AIAA/ASME/SAE/ASEE Joint Propulsion Conf. and Exhibit*, Cleveland, OH, July 13–15, 1998.

[6] M. Vahdati & M. Imregun, Non-linear aeroelasticity analyses of a fan blade using unstructured dynamic meshes, *Proc. of the Institution of Mechanical Engineers*, Part C, Mechanical Engineering Science, *210*(6), 1996, 549–564.

Biographies

Ng Khai Ching is currently working as a research assistant in the Department of Mechanical Engineering, Universiti Tenaga Nasional (UNITEN), Malaysia. He obtained his B.Eng. in mechanical engineering from UNITEN in 2003. His current research interests are computational fluid dynamics (CFD), numerical computing, and CAE software development.

Mohd. Zamri Yusoff is currently deputy dean of the College of Engineering, UNITEN. He obtained his Ph.D. in mechanical engineering from the University of Birmingham, UK, in 1997. His research interests are in CFD, numerical modelling, condensation, and other energy-related studies.

Talal F. Yusaf is currently associate professor at UNITEN. He obtained his Ph.D. in mechanical engineering from Universiti Kebangsaan Malaysia (UKM), Malaysia. His areas of specializations are biotechnology and combustion.